

Supporting Information

Recyclable surfactant containing dynamic covalent bond and relevant smart emulsions

Pei Liu,¹ Junhui Wu,¹ Xiaomei Pei,^{1,*} Zhenggang Cui,^{1,*} Jianzhong Jiang,¹ Binglei Song,¹ and Bernard P. Binks^{2,*}

¹ *The Key Laboratory of Synthetic and Biological Colloids, Ministry of Education,
School of Chemical and Material Engineering, Jiangnan University,
1800 Lihu Road, Wuxi, Jiangsu 214122, P.R. China*

² *Department of Chemistry, University of Hull,
Hull. HU6 7RX. U.K.*

No. Pages: 23

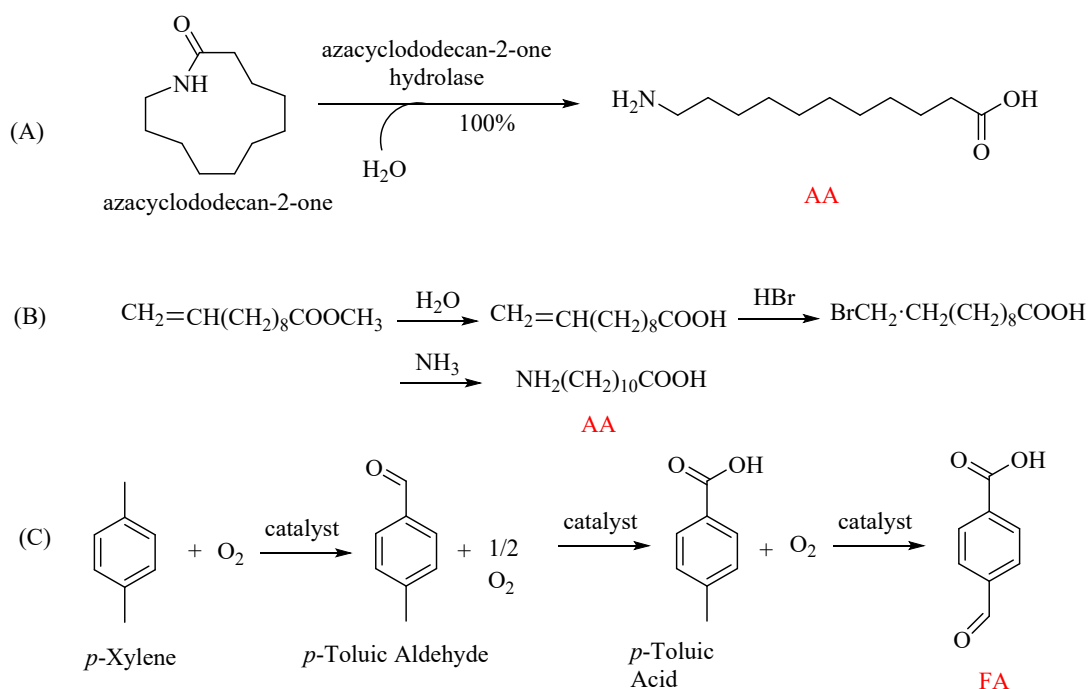
No. Figures: 27

No. Schemes: 1

EXPERIMENTAL

1. Materials

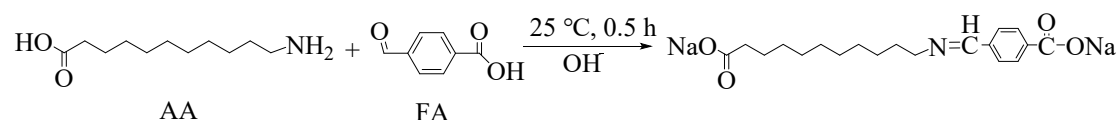
12-aminolauric acid ($C_{12}H_{25}NO_2$, AA > 98%), 4-formylbenzoic acid ($C_8H_6O_3$, FA > 98%) and *n*-decane ($C_{10}H_{22}$ > 98%) were purchased from Aladdin (Shanghai). AA can be synthesized both enzymatically and chemically as shown below by pathways (A)^[1] and (B)^[2] and FA can be synthesized chemically as shown by pathway (C).^[3] Hydrophilic silica (SiO_2) nanoparticles (HL-200, 99.8%) with a primary particle diameter of 20 nm and a BET surface area = 200 ± 20 m²/g were provided by Wuxi Jinding Longhua Chemical Co., China. Hydrophilic alumina (Al_2O_3) nanoparticles with a purity > 99.8%, a primary diameter of 13 nm and a BET surface area of 85-115 m²/g were purchased from Sigma. The SEM and TEM images of both types of particle are shown in Figure S11 and Figure S19, respectively. Other chemicals used were all analytically pure and purchased from Sinopharm Chemical Reagent Co. (Shanghai). Pure water with a pH close to 6.1 and a resistance of 18.2 M Ω cm was produced from a Simplicity Pure Water System (Merck Millipore, Shanghai). All chemicals were used as received unless specified otherwise.



- [1] Y. Fukuta, H. Komeda, Y. Yoshida, Y. Asano, High yield synthesis of 12-aminolauric acid by "enzymatic transcrystallization" of ω -laurolactam using ω -laurolactam hydrolase from *acidovorax* sp. T31. *Biosci. Biotechnol. Biochem.* **2009**, 73, 980-986.
- [2] Z. S. Petrović, Polymers from biological oils. *Contemp. Mater.* **2010**, 1, 39-50.
- [3] R. Shih, A. Bhattacharyya, C. J. Stevens, J. T. Walenga, Oxidation and crystallization process for aromatic carboxylic acid production. **2016**, US20140171679 A1.

2. Synthesis of Bola-form compound FA-AA

10 mmol of FA and AA were added to 100 mL NaOH aqueous solution ($\text{pH} = 12.00 \pm 0.02$) and the mixture was stirred for half an hour to ensure complete reaction. The Bola-form compound FA-AA was produced by formation of the dynamic covalent bond ($\text{C}=\text{N}$) as shown below:



Scheme S1. Formation of FA-AA from AA and FA *via* dynamic covalent bond.

3. Characterization of FA-AA

To confirm the chemical structure of the synthesized FA-AA, ESI-MS, ^1H NMR and FT-IR spectra were obtained and shown in Figures S1, S2 and S3, respectively.

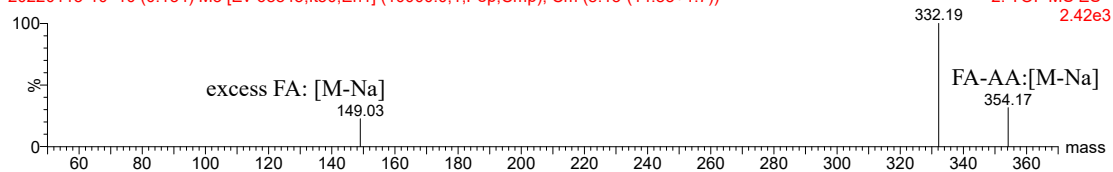
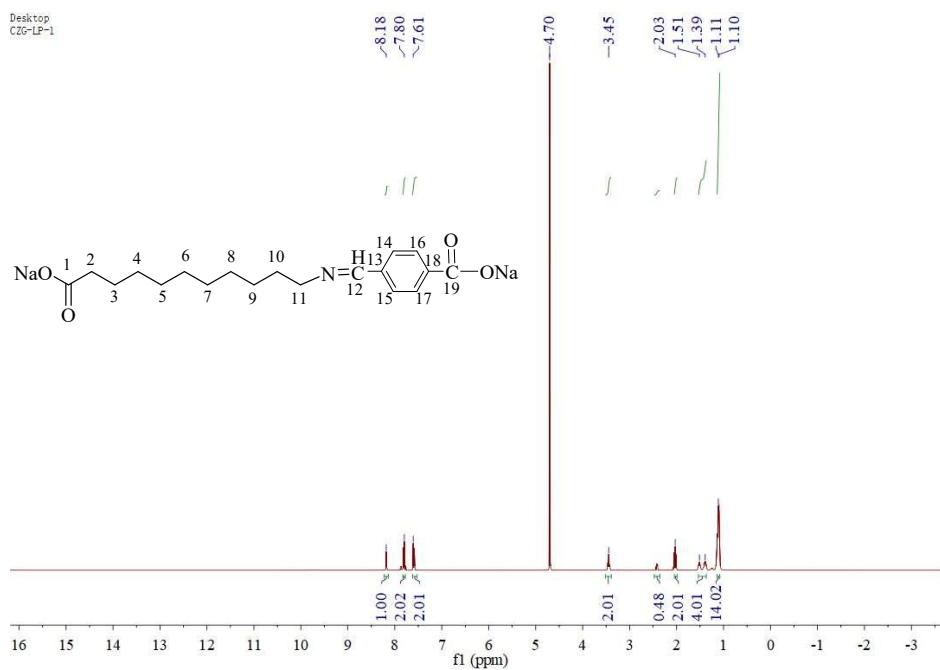
(i) ESI-MS characterization: ESI-MS spectrum was measured by an ultra-performance liquid chromatography-tandem mass spectrometer (LCZ/2690XE/ 996, Waters, USA). Pure water was used as the solvent.

(ii) ^1H NMR characterization: ^1H NMR spectra were measured by a Bruker spectrometer (Advance III, 400 MHz). D_2O /DMSO was used as the deuterated solvent.

(iii) FT-IR characterization: FTIR spectra were measured by a Fourier transform infrared spectrometer (Nicolet 6700, USA). Spectra with baseline correction were acquired.

CZG-LP-3

20220113-10 10 (0.134) M3 [Ev-68845,lt50,En1] (10000.0,1,Pep,Cmp); Cm (8:13-(14:83+1:7))

**Figure S1.** ESI-MS spectrum of synthesized FA-AA.**Figure S2.** ¹H NMR spectrum of FA-AA (60 mM FA and 60 mM AA as reactants, pH = 12) in D₂O.

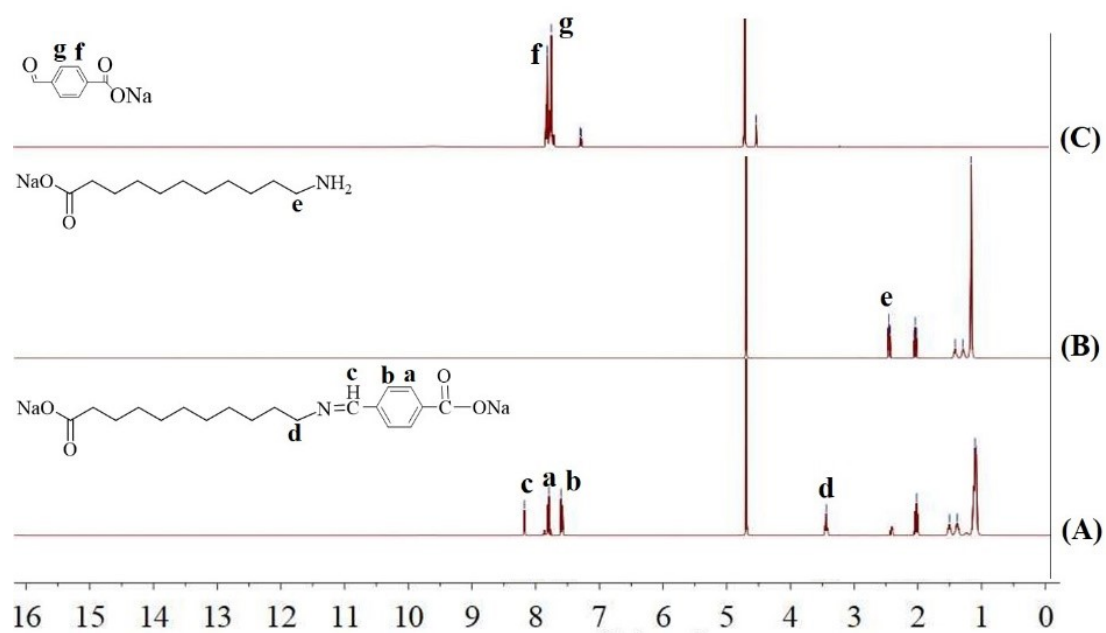


Figure S3. ^1H NMR spectra of (A) FA-AA (60 mM FA and 60 mM AA as reactants, pH = 12), (B) AA (60 mM, pH = 12) and (C) FA (60 mM, pH = 12) in D_2O .

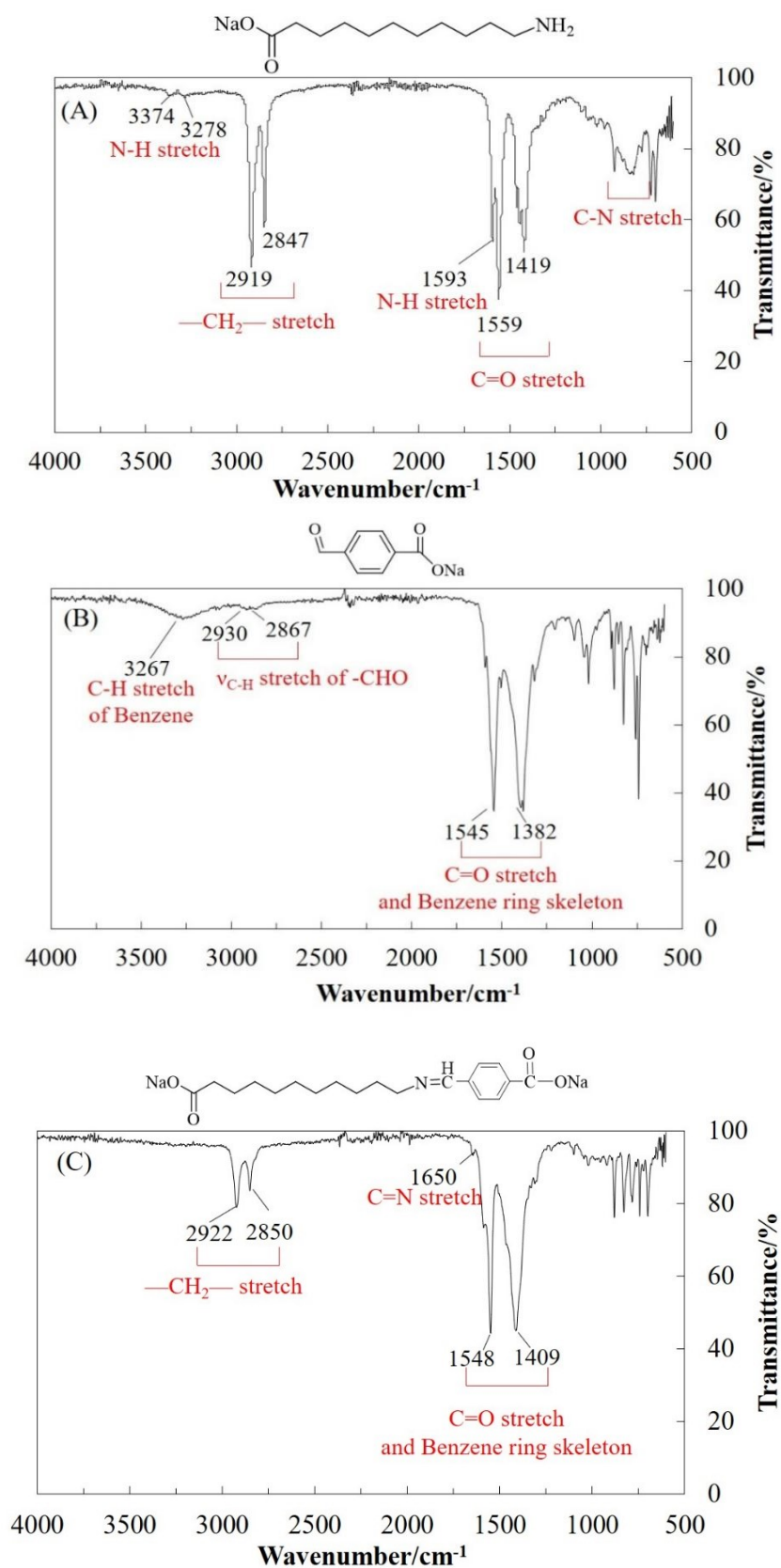


Figure S4. FTIR spectra of (A) AA, (B) FA and (C) FA-AA at pH = 12.

The ESI-MS spectrum shown in Figure S1 (negative ion mode) indicates an m/z of $332.19 = [M-2Na+H]^-$ and an m/z of $354.17 = [M-Na]^-$. Probably, FA is in slight excess thus resulting in an m/z of $149.03 = [M-Na]^-$.

The 1H NMR data shown in Figure S2 indicates a total hydrogen number of 25, in good agreement with the molecular formula of FA-AA. 1H NMR (400 MHz, D_2O , δ): 8.22 – 8.14 (s, C12-1H), 7.83 – 7.77 (s, C16-2H, C17-2H), 7.62 – 7.52 (s, C14-2H, C15-2H), 3.52 – 3.39 (s, C11-2H), 2.05 – 1.99 (s, C2-2H), 1.53 – 1.37 (d, $J = 49.4$ Hz, C3-2H, C10-2H), 1.13 – 1.08 (d, $J = 6.2$ Hz, C4-2H, C5-2H, C6-2H, C7-2H, C8-2H, C9-2H). Compared with the 1H NMR spectra of FA and AA shown in Figure S3, the spectrum of FA-AA showed a new peak at 8.18 ppm, corresponding to hydrogen at position (c) in FA-AA. Besides, the hydrogen peak at position (e) in AA moves downfield to position (d) in FA-AA due to the electron-attracting effect of the $C=N$ group and $COONa$ group. The chemical shift of the hydrogen peak on the benzene ring skeleton is also slightly affected.

The FTIR spectrum is shown in Figure S3 (C). The strong peaks at 2922 cm^{-1} and 2850 cm^{-1} are stretching vibrations of methyl and methylene groups ν_{C-H} ; the broad absorbance peaks at 1548 cm^{-1} and 1409 cm^{-1} are the stretching vibrations of $\nu_{C=O}$ coupling in carboxylate, which has overlapped with the benzene ring skeleton vibration. Compared with the spectrum of AA (A), the symmetric and asymmetric stretching vibration absorption peaks of ν_{N-H} at 3347 cm^{-1} and 3278 cm^{-1} , bending vibration absorption peak of δ_{N-H} at 1593 cm^{-1} and broad bending vibration absorption peak of ω_{N-H} at $910\text{-}750\text{ cm}^{-1}$ in the spectrum of FA-AA disappeared. In addition, the stretching vibration of $\nu_{C=N}$ at 1650 cm^{-1} also showed that FA-AA was successfully synthesized.

To further confirm the successful synthesis of FA and AA intuitively, the silver mirror reaction was conducted as shown in Figure S5. As shown in number ⑥ (AA⁻), a silver mirror was generated due to the reaction of the aldehyde group with silver ammonia solution. However, no similar phenomenon except a slight blackening was observed in number ⑤ (FA-AA). This could be caused by unreacted or excess FA. This further shows that FA-AA can be successfully generated by simple stirring at room

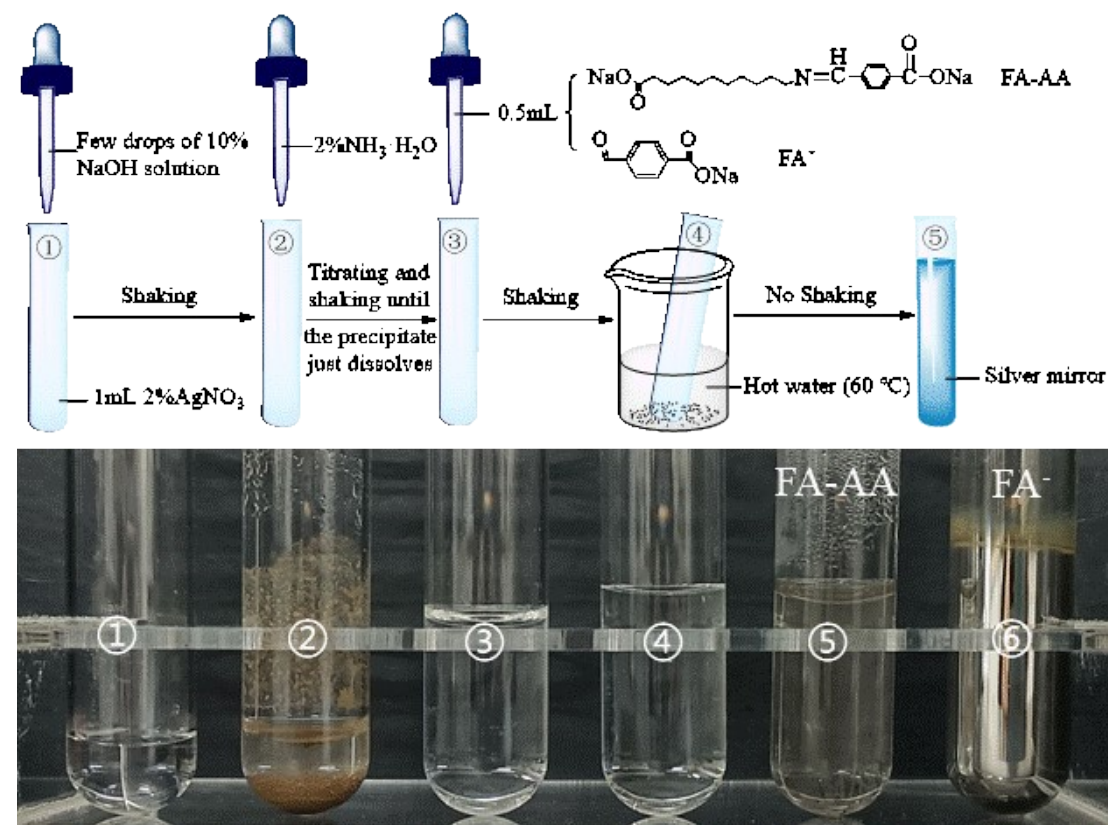


Figure S5. Examination of aldehyde group in compounds FA-AA and FA⁻ using freshly prepared silver nitrate.

4. Preparation of emulsions

4.1 Conventional emulsions

3 mL of H⁺AA aqueous solution was added into a 10 mL glass vessel of dimensions 22 mm (d) × 52 mm (h), followed by addition of 3 mL of *n*-decane and the mixture was homogenized using an Ultra-Turrax homogenizer (IKA T18 basic, S18N-10G head) at 11,000 rpm for 2 min. The concentration of surfactant is expressed as mM with respect to the aqueous phase and the oil:water volume ratio was fixed at 1:1.

4.2 Pickering emulsions and oil-in-dispersion emulsions

Silica nanoparticles (0.1 wt.%) or alumina nanoparticles (0.01 wt.%) were dispersed in 3 mL of surfactant solution using an ultrasonic probe and then equal volumes of *n*-decane were added. The mixture was then homogenized using an Ultra-

Turrax homogenizer at 11,000 rpm for 2 min. The oil:water volume ratio was fixed at 1:1 and the emulsion type and stability were identified and monitored as described above.

5. Characterization of emulsions

5.1 Emulsion type and stability

The type of emulsion was determined by the drop test and staining/positive fluorescence microscope (Nikon 80i, Nikon Co.). Nile red was used to color the oil. Emulsion stability was monitored by taking photographs at different times using a digital camera and optical micrographs using a microscope system (VHX-1000, Keyence Co.), respectively.

5.2 Field emission scanning electron microscopy

A drop of the prepared emulsion was spread on a clean dry silicon wafer, which was then moved inside an incubator to dry at 25 °C. The silicon wafer with the dried sample was fixed on the specimen stage of the SEM instrument (S-4800, Hitachi Ltd.) using a conductive adhesive, and the sample was sputter coated with gold and analyzed at an acceleration voltage of 3 kV.

5.3 Ultra-depth three-dimensional microscopy

A small amount of emulsion was added dropwise on a clean glass slide at 25 °C. After complete evaporation of water and *n*-decane, optical micrographs of the residue were taken.

6. pH-responsive behavior of emulsions

To observe pH-responsive behavior, about 50 µL of concentrated HCl solution (2 M) or concentrated NaOH solution (2 M) was added to an emulsion to adjust the pH of the aqueous phase to 4 and 12 respectively, followed by homogenization (11,000 rpm for 2 min for preparing emulsion) or by stirring/shaking (for demulsification).

7. Measurements

7.1 pK_a

An aqueous solution of AA⁻ at 3 mM was prepared and its pH was adjusted to 12

by adding solid NaOH directly. Then, a potentiometric method was used to determine the pK_a . 0.2 M HCl solution was added dropwise in steps of 50 μ L until the pH reached 2.6. Each pH value was recorded at 25 $^{\circ}$ C. Curves of pH *versus* volume of HCl solution added were plotted and its first derivative was calculated as the dpH/dV -V curve.

7.2 Surface tension/interfacial tension

The surface tensions of aqueous solutions were measured by the du Noüy method using a home-built instrument at 25 ± 0.2 $^{\circ}$ C. The interfacial tension was measured on an interfacial tensionmeter (OCA 40, Dataphysics, Germany). To prepare surfactant solutions, equimolar amounts of AA and hydrochloric acid were dissolved in pure water and diluted to 100 mL in a flask. The pH (H^+AA aqueous solution) was measured to be 3.96. Similarly, the pH of AA^- and FA-AA was determined to be 12.03 and 12.05 respectively. They were then diluted using either an aqueous solution of HCl at pH = 4.0 or an aqueous solution of NaOH at pH = 12.0 to different concentrations. The pH of the solutions was measured using a digital pH meter (FE220, Mettler Toledo) at room temperature (20-25 $^{\circ}$ C). Before measurement, the surfactant solution was transferred to a clean petri dish with diameter of 60 mm and allowed to stand for 24 h at 25 ± 0.1 $^{\circ}$ C (air thermostat). The surface tensions and interfacial tensions were all measured at least three times and the average value is reported.

7.3 Zeta potential

A series of H^+AA solutions of different concentration containing silica nanoparticles (0.1 wt.%) or Al_2O_3 nanoparticles (0.01 wt.%) were prepared using an ultrasonic probe and equilibrated in an incubator at 25 $^{\circ}$ C for 24 h. The zeta potentials were measured using a Brookhaven Zeta PLAS instrument. The average error is ± 0.5 mV.

7.4 Adsorption of surfactant at silica particle-water interface

The adsorption isotherm of surfactant H^+AA at the particle-water interface was measured by the depletion method. Silica nanoparticles (0.1 wt.%) were dispersed in aqueous surfactant solutions of different concentration for 24 h at 25 $^{\circ}$ C to reach equilibrium. The surface tension of the dispersion (0.1 wt.% silica + H^+AA^+) was then measured by the du Noüy ring method. The equilibrium concentration of surfactant was

calculated from the surface tension of the solution without particles as calibration.

7.5 Contact angle

The oil-water-glass contact angles were measured using an optical contact angle analyzer (OCA 40, Dataphysics, Germany) through the inverted sessile drop method where an oil (*n*-decane) droplet of 0.5 μL was first released through a U-shaped needle into the aqueous solution and then captured by the underside of the glass slide. The glass slide had been immersed in aqueous solutions of different surfactant concentration in advance for adequate adsorption or contact.

7.6 UV absorbance

The absorbance of aqueous FA-AA solutions of different concentration at 200-800 nm was scanned to find the wavelength at which maximum absorption (λ_{max}) was achieved. Then, the absorbance of all the prepared solutions at λ_{max} was measured to obtain an absorbance-concentration calibration curve. After demulsification, the absorbance of the separated aqueous phase (without nanoparticles) and *n*-decane was measured and compared with that of fresh oil. Any increase/decrease in absorbance of the aqueous/oil phase suggests transfer of FA-AA from water to oil.

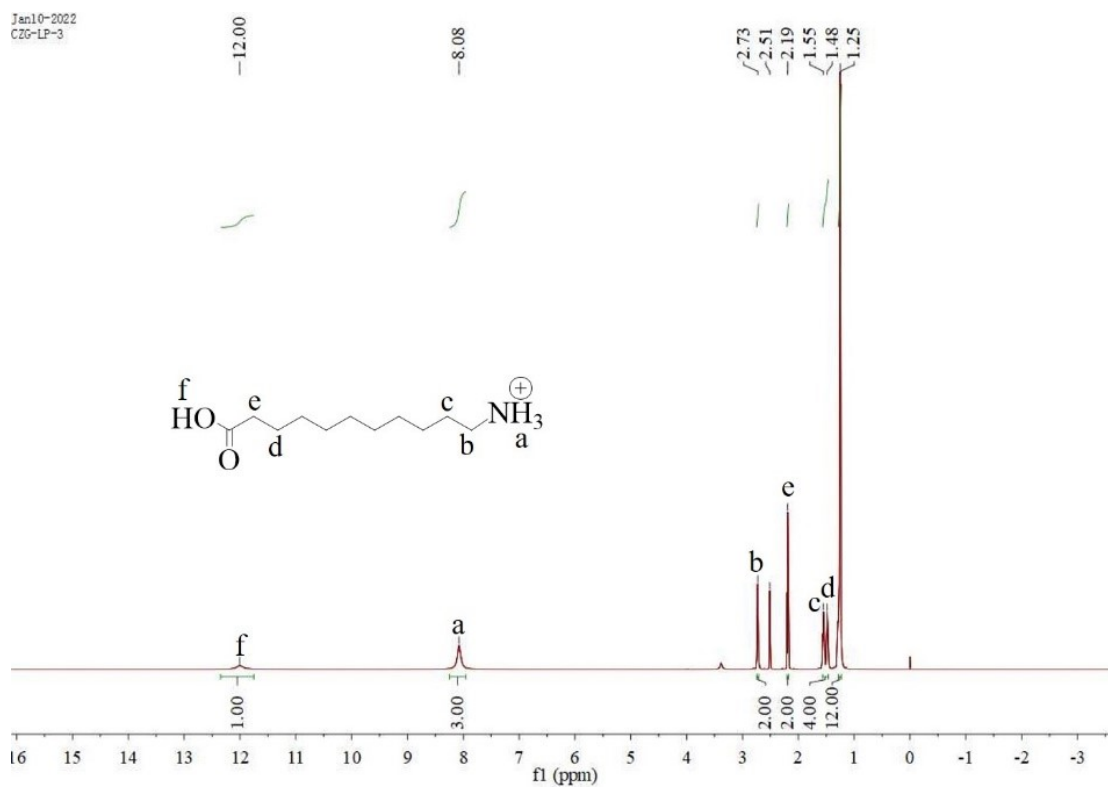


Figure S6. ^1H NMR spectrum of H^+AA (60 mM, pH = 4) in DMSO.

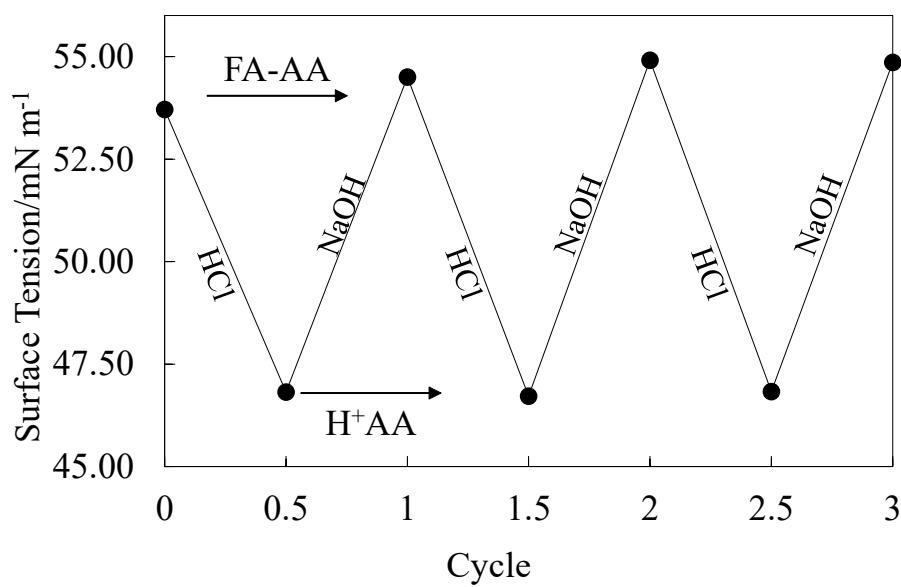


Figure S7. Surface tension of 20 mM aqueous FA-AA following alternate addition of HCl (pH = 4) and NaOH (pH = 12).

$$\delta_0(AA^-)$$

$$= \frac{K_{a1}K_{a2}}{[H^+]^2 + [H^+]K_{a1} + K_{a1}K_{a2}} = \frac{10^{-pK_{a1}}10^{-pK_{a2}}}{[10^{-pH}]^2 + 10^{-pH}10^{-pK_{a1}} + 10^{-pK_{a1}}10^{-pK_{a2}}}$$

$$\delta_1(H^+AA^-)$$

$$= \frac{[H^+]K_{a1}}{[H^+]^2 + [H^+]K_{a1} + K_{a1}K_{a2}} = \frac{10^{-pH}10^{-pK_{a1}}}{[10^{-pH}]^2 + 10^{-pH}10^{-pK_{a1}} + 10^{-pK_{a1}}10^{-pK_{a2}}}$$

$$\delta_2(H^+AA)$$

$$= \frac{[H^+]^2}{[H^+]^2 + [H^+]K_{a1} + K_{a1}K_{a2}} = \frac{[10^{-pH}]^2}{[10^{-pH}]^2 + 10^{-pH}10^{-pK_{a1}} + 10^{-pK_{a1}}10^{-pK_{a2}}}$$

$$\delta_0 + \delta_1 + \delta_2 = 1$$

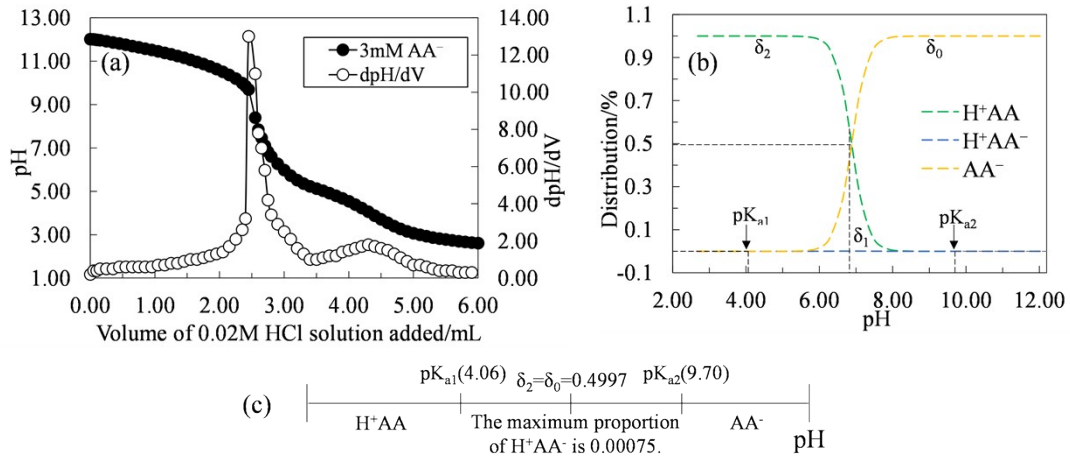


Figure S8. (a) pH titration curve of 3 mM H⁺AA solution and corresponding dpH/dV curve at 25 °C, (b) distribution of components in solution as a function of pH, (c) illustration of the predominant component in solution at different pH ranges derived from the pH titration curve. The mole fraction (δ) of different components (H⁺AA, H⁺AA⁻, AA⁻) was calculated using the equations above the figure.

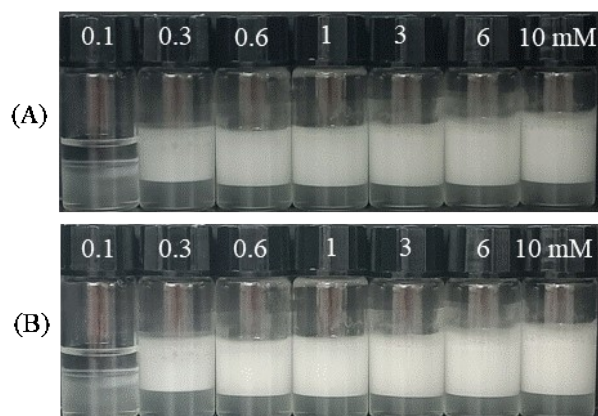


Figure S9. (A and B) Digital photos of *n*-decane-in-water (3 mL/3 mL) conventional emulsions stabilized by AA⁻ dissolved in alkaline water (pH = 12.0) at different concentrations (given), taken (A) immediately and (B) 24 h after preparation at 25 °C.

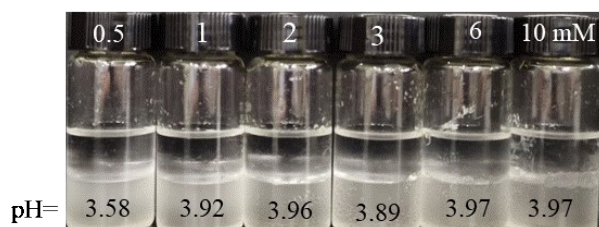


Figure S10. Digital photos of *n*-decane-in-water (3 mL/3 mL) conventional emulsions stabilized by FA-AA at different concentrations (given), taken immediately after preparation at 25 °C. FA-AA was initially dissolved in alkaline water (pH = 12.0) followed by addition of HCl to make the solution acidic (pH < 4).



Figure S11. Digital photos of *n*-decane-in-water (7 mL/7 mL) conventional emulsions stabilized by (1) H^+AA at $\text{pH} = 4$, (2) AA^- (original $\text{pH} = 12$ but was reduced to $\text{pH} = 4$ by addition of HCl), (3) FA-AA (original $\text{pH} = 12$ but was reduced to $\text{pH} = 4$ by addition of HCl) all at 6 mM taken immediately after preparation at 25 °C.

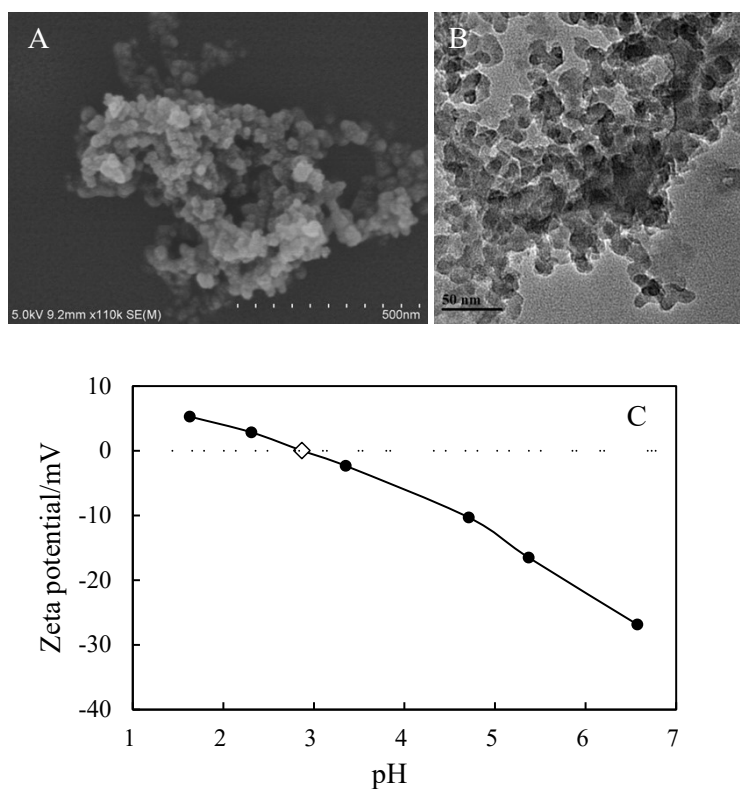


Figure S12. (A) SEM and (B) TEM images of silica nanoparticles, (C) zeta potential of 0.1 wt.% silica nanoparticles dispersed in water of different pH at 25 °C.

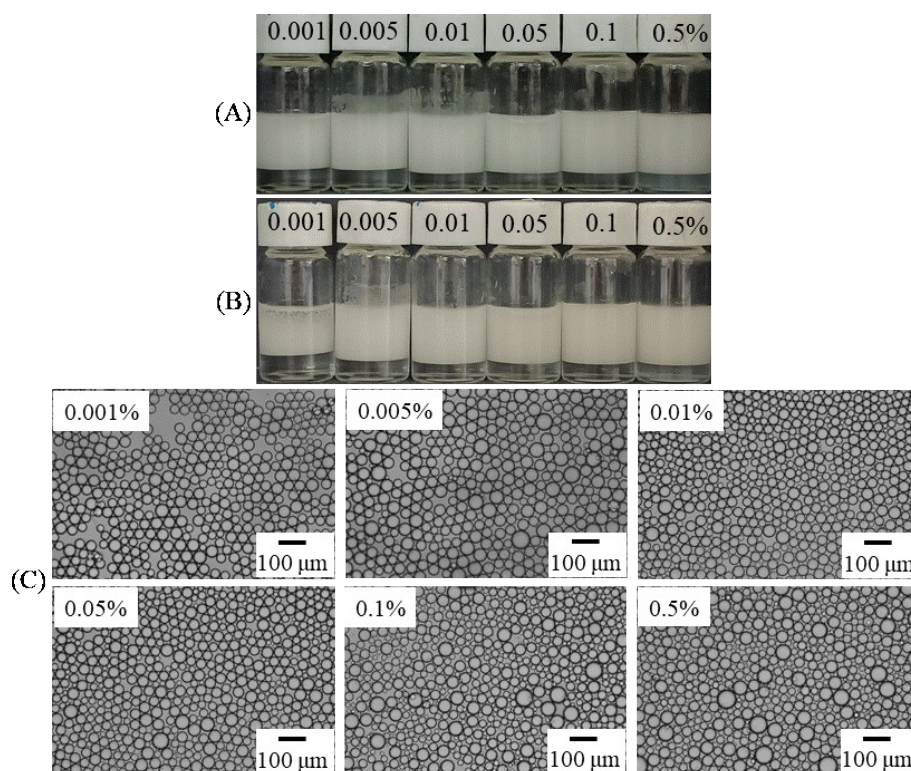


Figure S13. (A and B) Digital photos of *n*-decane-in-water (3 mL/3 mL) Pickering emulsions stabilized by silica nanoparticles at different concentrations (wt.%) in combination with 0.6 mM H⁺AA surfactant, taken (A) immediately and (B) 24 h after preparation. (C) Micrographs of emulsions corresponding to (B).

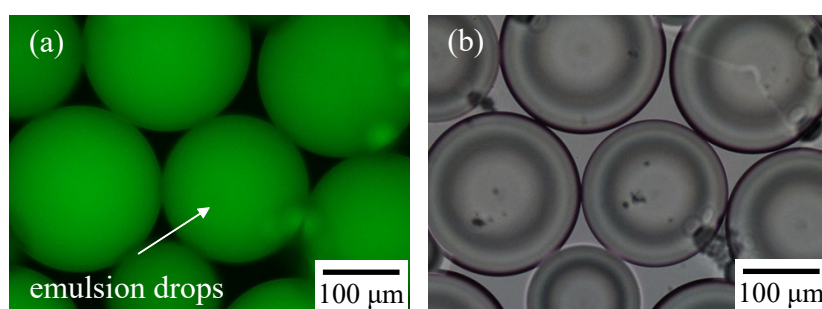


Figure S14. Fluorescence microscopy images of *n*-decane-in-water Pickering emulsion stabilized by 0.1 wt.% silica nanoparticle in combination with 0.06 mM H⁺AA at pH = 4 with the oil phase stained with Nile red. (a) Dark-field with green excitation filter and (b) bright-field.

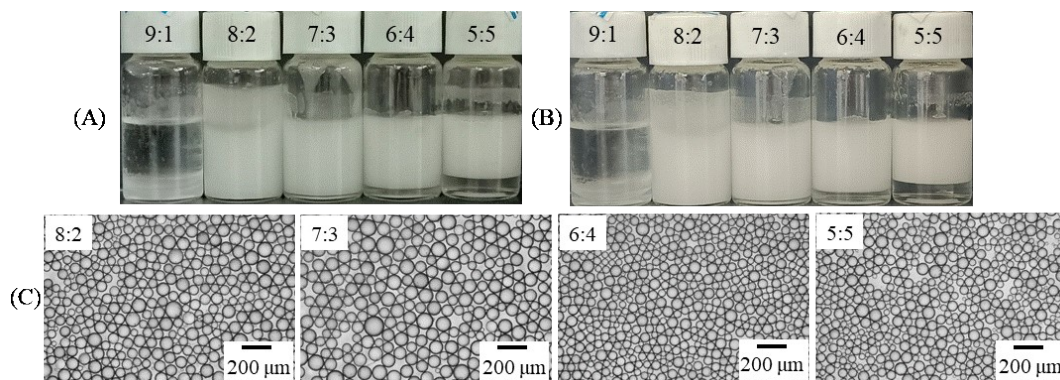


Figure S15. (A and B) Digital photos and (C) corresponding optical micrographs of *n*-decane-in-water Pickering emulsions stabilized by 0.1 wt.% silica nanoparticles in combination with 0.6 mM H⁺AA at different oil:water ratios as shown, taken (A) immediately and (B, C) 24 h after preparation.

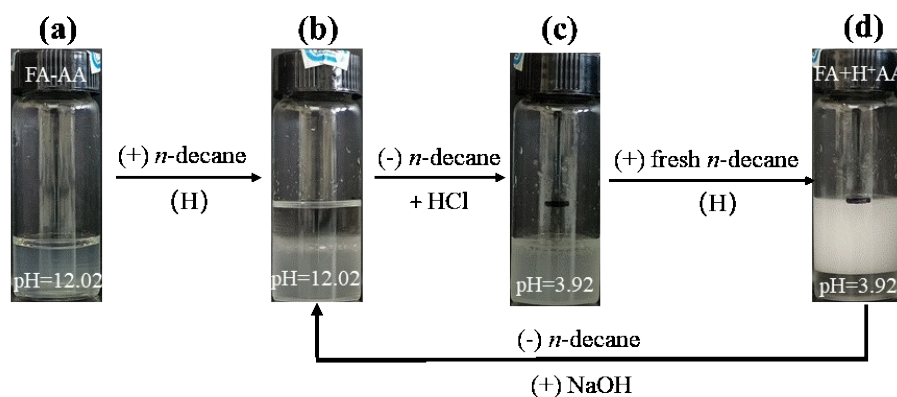


Figure S16. Digital photos of *n*-decane-in-water (7 mL/7 mL) Pickering emulsions stabilized by 0.1 wt.% silica nanoparticles and 0.6 mM FA-AA undergoing switching on/off cycle induced by adding HCl/NaOH. (a) Initial 0.1 wt.% silica nanoparticle dispersion (alkaline), (b) add *n*-decane followed by homogenization (H), (c) remove separated oil and add HCl to make dispersion acidic, (d) add fresh *n*-decane followed by homogenization.

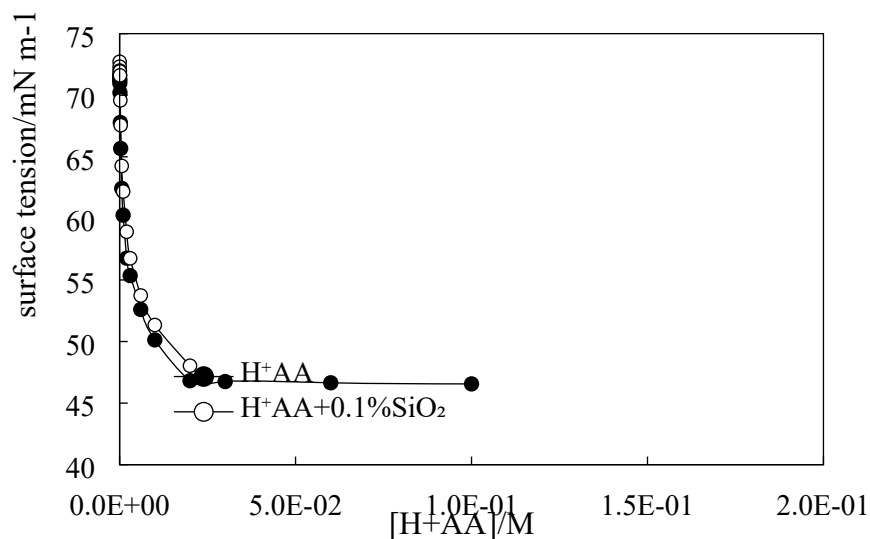


Figure S17. Surface tension of aqueous solutions of H⁺AA without and with 0.1 wt.% silica nanoparticles at pH = 4 as a function of initial surfactant concentration at 25 °C.

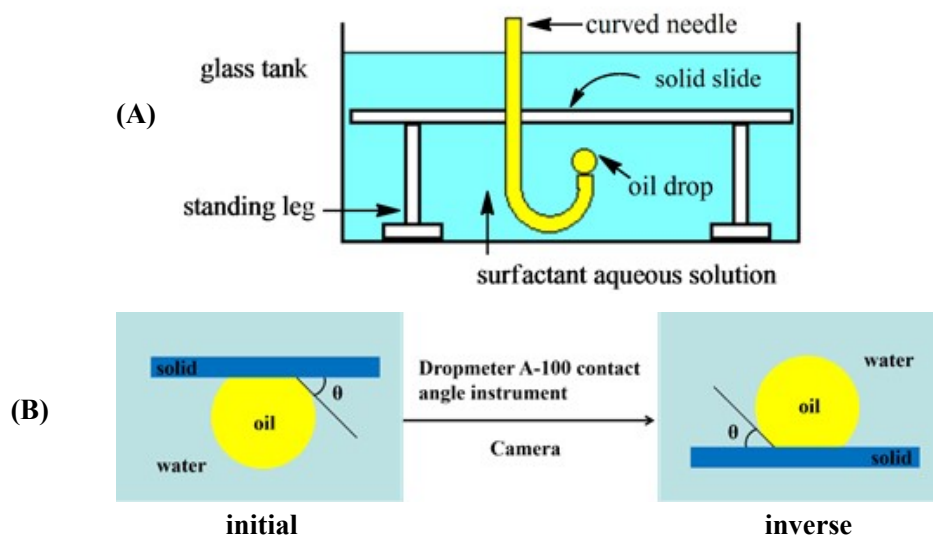


Figure S18. (A) Schematic diagram of apparatus for measuring contact angle and (B) side view of the inverted sessile drop using Dropmeter A-100 instrument.

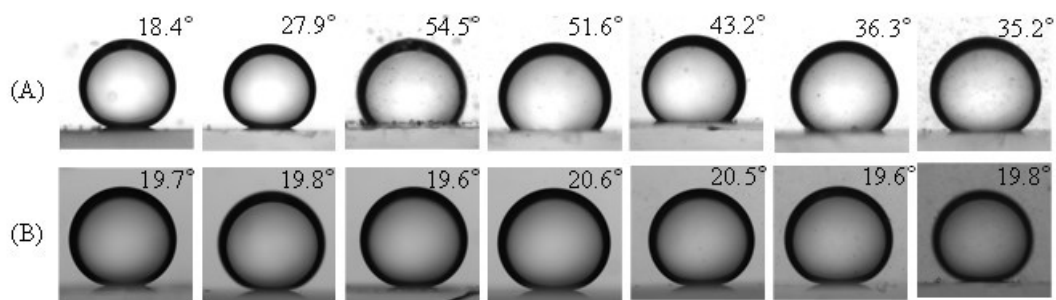


Figure S19. Images of sessile drops (inverted) of *n*-decane captured by glass slides immersed in aqueous solutions of (A) H^+AA (pH = 4) and (B) FA-AA (pH = 11-12) at different concentrations; numbers are contact angle of water (θ_w) measured at 25 °C. [surfactant] from left to right is: 0.01, 0.1, 1, 6, 10, 15, 20 mM.

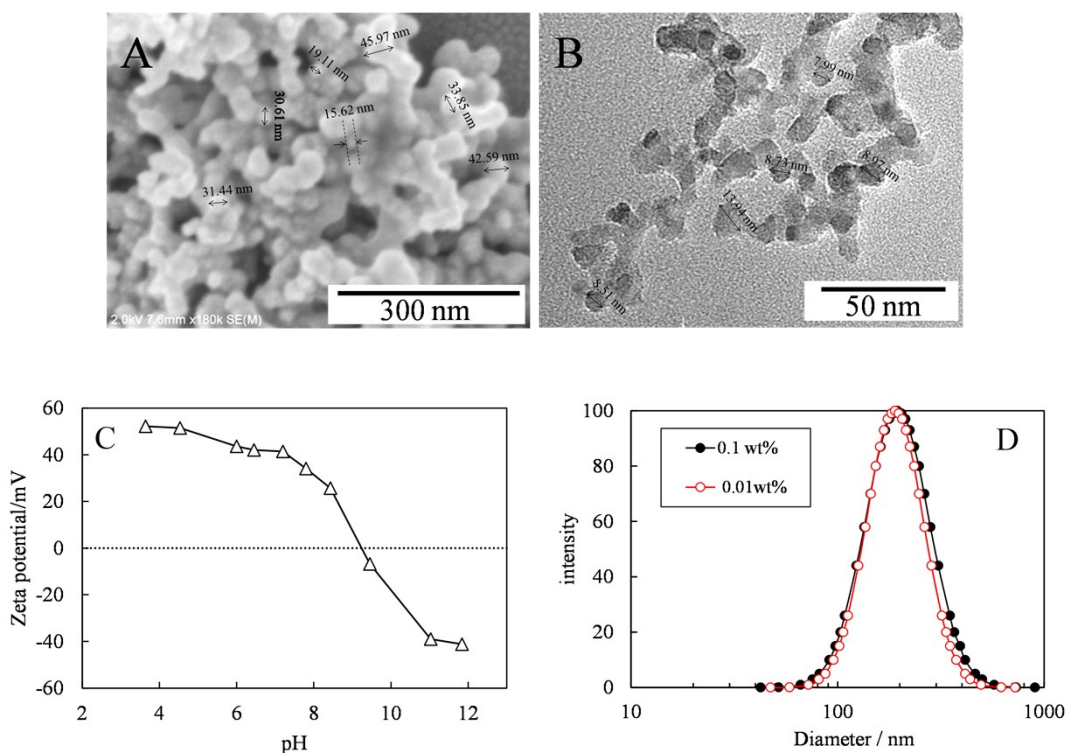


Figure S20. (A) SEM and (B) TEM images of alumina nanoparticles, (C) zeta potential of 0.1 wt.% alumina nanoparticles dispersed in water of different pH, (D) size distribution of alumina nanoparticles dispersed in neutral water at two concentrations as shown at 25 °C.

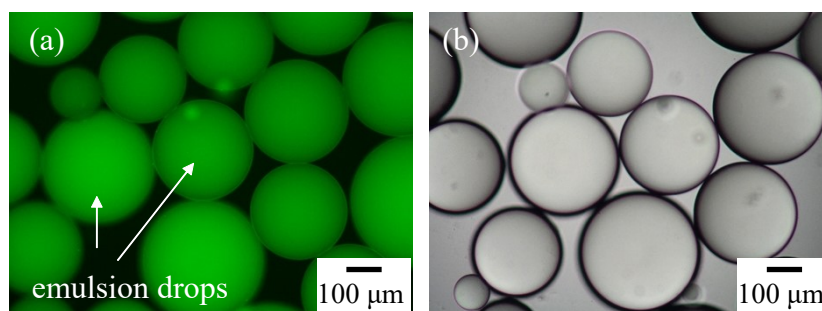


Figure S21. Fluorescence microscopy image of *n*-decane-in-dispersion emulsion stabilized by 0.06 mM H⁺AA in combination with 0.01 wt.% alumina nanoparticles at pH = 4 with the oil phase stained with Nile red. (a) Dark-field with green excitation filter and (b) bright-field.

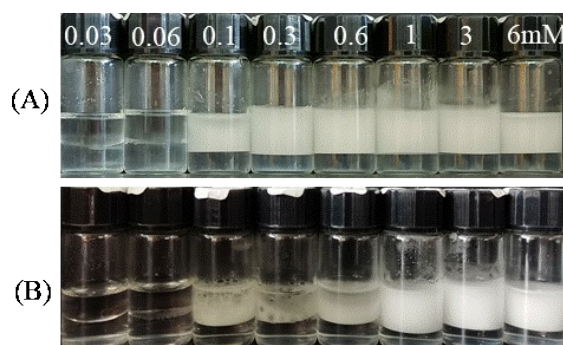


Figure S22. (A) Digital photos of *n*-decane-in-water (3 mL/3 mL) oil-in-dispersion emulsions stabilized by H⁺AA at different concentrations (given) and 0.01 wt.% alumina nanoparticles at pH = 4, taken (A) one month and (B) two months after preparation at 25 °C.

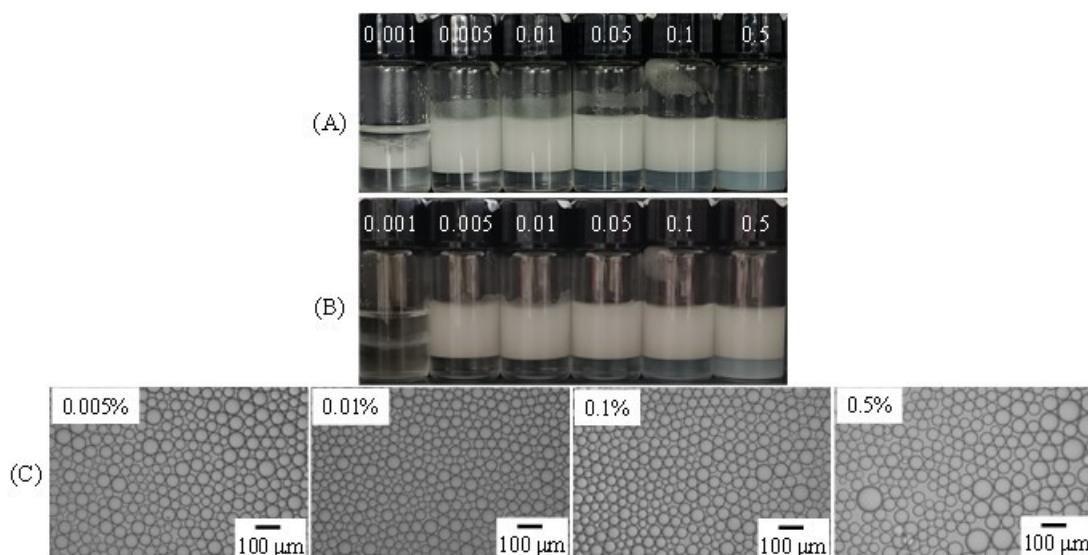


Figure S23. (A and B) Digital photos of *n*-decane-in-water (3 mL/3 mL) oil-in-dispersion emulsions stabilized by 0.06 mM H⁺AA surfactant in combination with alumina nanoparticles of different concentration (wt.% as shown) at pH = 4, taken (A) immediately and (B) 24 h after preparation. (C) Micrographs of emulsions corresponding to (B).

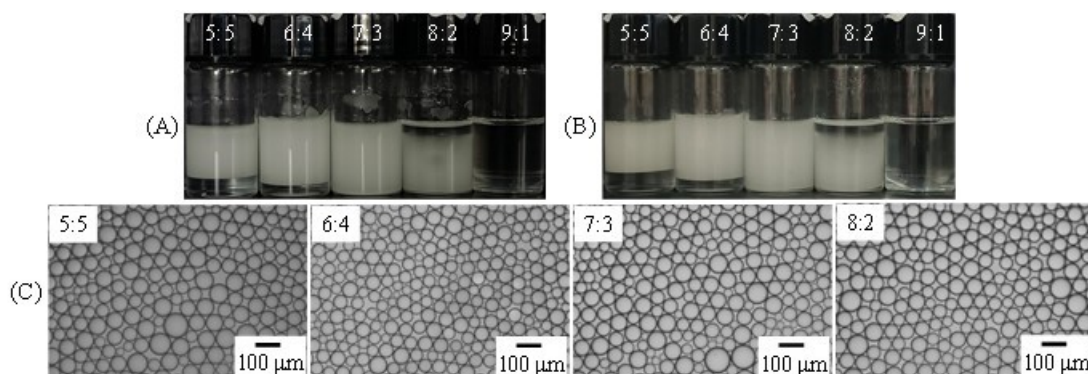


Figure S24. (A and B) Digital photos and (C) optical micrographs of *n*-decane-in-water (3 mL/3 mL) oil-in-dispersion emulsions with different oil:water volume ratios (as shown) stabilized by 0.06 mM H⁺AA in combination with 0.01 wt.% alumina nanoparticles at pH = 4, taken (A) immediately and (B, C) 24 h after preparation.

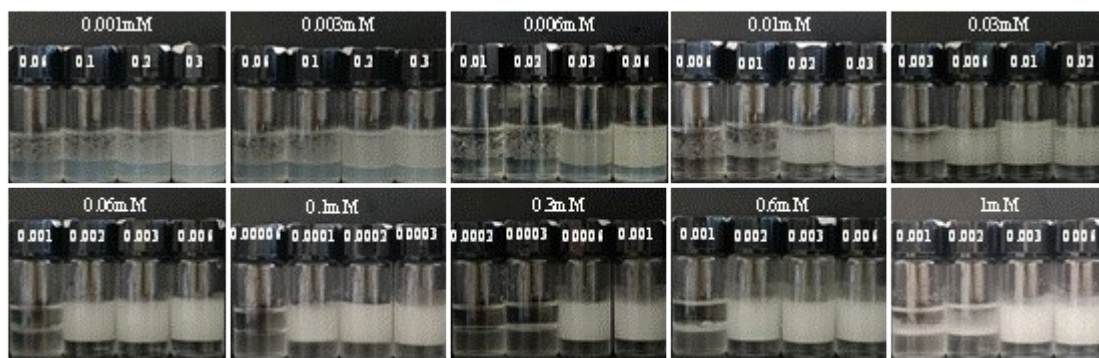


Figure S25. Digital photos of *n*-decane-in-water (3 mL/3 mL) oil-in-dispersion emulsions stabilized by H⁺AA in combination with minimum alumina particle concentration at pH = 4, taken 24 h after preparation. [alumina]/wt. % is shown above vessels.

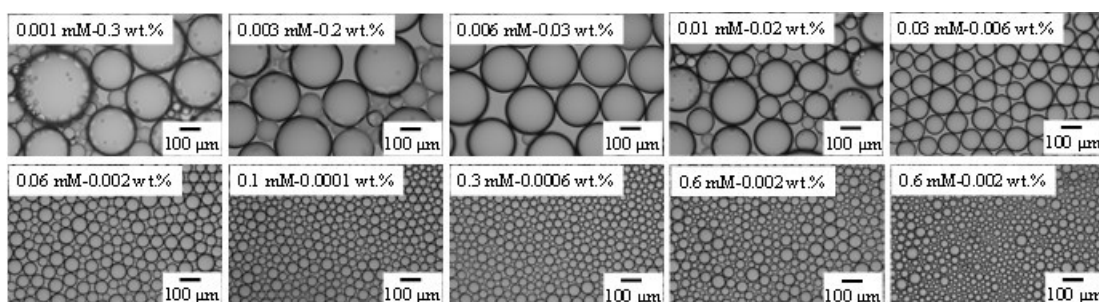


Figure S26. Optical micrographs of *n*-decane-in-water (3 mL/3 mL) oil-in-dispersion emulsions stabilized by H⁺AA of different concentrations in combination with the corresponding minimum concentration of alumina particles at pH = 4, taken 24 h after preparation. Concentrations of surfactant and particles are shown on the micrographs.

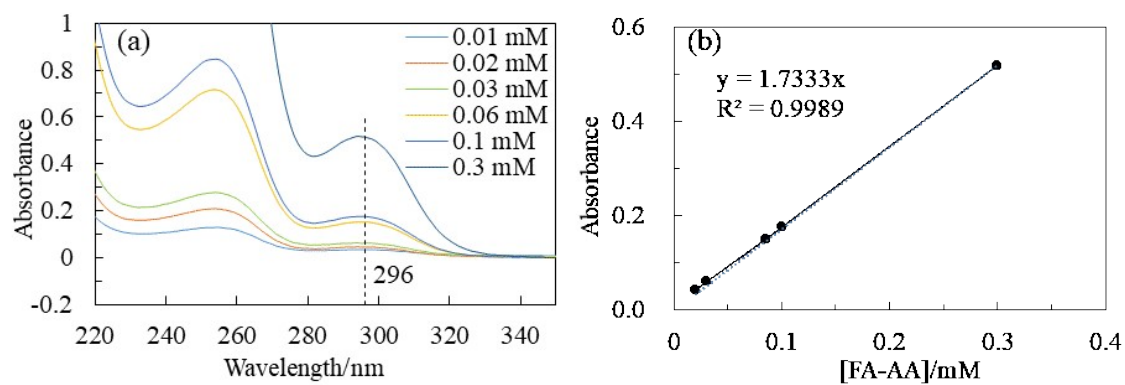


Figure S27. (A) Absorbance-wavelength scan and (B) absorbance-concentration plot at 296 nm for aqueous solutions of FA-AA at pH = 12 at 25 °C.